Bias in the paleoceanographic time series: Tests with a numerical model of U, C_{org}, and Al burial

Y. Donnadieu,[1] P. Lecroart, P. Anschutz, and P. Bertrand
DGO-UMR 5805, Université Bordeaux 1, Talence, France

Received 8 March 2001; revised 16 April 2002; accepted 16 April 2002; published 13 August 2002.

[1] We have constructed a nonsteady state numerical model of organic carbon, aluminum, and uranium burial to examine the dynamic response of sediments to variations on thousand years scale. The three components are defined by distinct behaviors in the sedimentary system. The aluminum is a conservative component, the organic carbon is a nonconservative component degraded in superficial sediment, and the uranium is a component affected by redox conditions. By introducing a simultaneous variation of incoming fluxes of C_{org} and Al, geochemical profiles of Al, C_{org}, and U clearly show separate distributions after burial. Each component record the synchronous variation of the incoming fluxes, but the position in the sedimentary pile of the recording differs from a component to another. We show that a minimum of U could be linked to a rapid ascent of the oxic front during an increase in C_{org} flux. *INDEX TERMS:* 4267 Oceanography: General: Paleoceanography; 4804 Oceanography: Biological and Chemical: Benthic processes/benthos; 4808 Oceanography: Biological and Chemical: Chemical tracers; 4842 Oceanography: Biological and Chemical: Modeling; 4863 Oceanography: Biological and Chemical: Sedimentation; *KEYWORDS:* time lag, sedimentary system, high-resolution record, modeling, bioturbation

1. Introduction

[2] Sediments, which are the ultimate repository of biogenic or detrital particles, constitute the historical record of past events in the oceans. However, in order to accurately interpret the sedimentary record we have to distinguish the primary signals registered at the water-sediment interface from postdepositional changes. These changes, which take place during the early diagenesis, include the extensive chemical and physical transformations that occur close to the sediment-water interface. When reactive organic matter settles on the seafloor, it provokes a sequence of reactions that remove organic carbon from the sediment system. Organic carbon oxidation occurs through a well-defined sequence of consumption of terminal electron acceptors. Oxygen is consumed first, followed by nitrate, manganese oxide, reactive iron oxides, sulphate, and finally oxygen bound in organic matter [*Froelich et al.*, 1979].

[3] The fundamental objective of paleoceanographic studies is to reconstitute the temporal evolution of oceanographic parameters such as sea surface temperature, primary productivity or bottom water oxygen concentration from sedimentary cores. Depth in the sediment is considered as a measure of time since deposition. However, nearly all particles that reach the floor of the ocean are displaced several times by animals before they are buried to become part of the sedimentary system [*Wheatcroft*, 1992]. This mixing of sediment, called bioturbation, has profound effects on a wide range of mineralogical, paleontological, and chemical parameters [*Berger and Health*, 1968; *Guinasso and Schink*, 1975; *Bard et al.*, 1987; *Aller*, 1990; *Jorissen et al.*, 1995]. It can bias dating scales of paleoceanographic records in different ways for each measured signal, because bioturbation rates are particle size-dependent [*Wheatcroft*, 1992].

[4] Moreover, at a given level in a sedimentary record, the different signals (trace and major elements, isotopes, microfossils) are commonly considered to be synchronous. But geochemical profiles in recent sediments clearly show that the accumulation of redox sensitive compounds used in paleoceanography such as Mo, U, Re [*Barnes and Cochran*, 1993; *Calvert and Pedersen*, 1993; *Colodner et al.*, 1995; *Crusius et al.*, 1996] or Mn, Cd [*Aller*, 1990; *Rosenthal et al.*, 1995; *Gobeil et al.*, 1997; *Morford and Emerson*, 1999] takes place below the sediment-water interface. For a given lithology, the depth where a tracer is fixed results from a balance between diffusion rates of components produced or consumed within the interstitial waters, and biological mixing. Thus it is likely that the dating scales derived from such components could be different from scales derived from the accumulation of conservative particles, e.g. Al. In order to improve our understanding of this phenomenon, we have developed a nonsteady state numerical model of organic carbon, aluminum, and uranium burial to simulate the down core geochemical record. There exists an extensive literature dealing with diagenetic modeling [*Berner*, 1980; *Middelburg*, 1989; *Rabouille and Gaillard*, 1991a, 1991b; *Van Cappellen et al.*, 1993; *Soetaert et al.*, 1996a, 1996b; *Boudreau*, 1997]. Most models have been developed to provide information on the amount of carbon degraded, mineralization rates, and fluxes through the sediment-water interface. But only a few attempts have been made to examine the dynamic response of sediments to variations on thousand year scales [*Dhakar and Burdige*, 1996; *Crusius et al.*, 1999]. Here, we present a new model,

[1] Now at Laboratoire des Sciences du Climat et de l'Environnement, UMR CNRS-CEA, CEA Saclay, Orme des Merisiers, Gif-sur-Yvett cedex, France.

0883-8305/02/2001PA000638

Table 1. Equations and Parameters Used in the Model

	Equations	Comments
(1.1)	$\frac{\partial G}{\partial t} = D_b \frac{\partial^2 G}{\partial z^2} - w\frac{\partial G}{\partial z} - k_1 G$	refers to the one-G model for the mixed layer. k_1 is a constant (yr^{-1}); w, sedimentation rate (cm yr^{-1}); G, C_{org} concentration; t, time (yr); z, depth (cm); D_b, bioturbation rate (cm^2 yr^{-1})
(1.2)	$\frac{\partial G}{\partial t} = -w\frac{\partial G}{\partial z} - k(t)G$	refers to the power law for the fossilized layer; k (yr^{-1}) is a function of time (log k = −log t − 0.84 with t = z/w)
(1.3)	$\frac{\partial Ox}{\partial t} = D_{ox}\frac{\partial^2 Ox}{\partial z^2} - w\frac{\partial Ox}{\partial z} - \gamma\frac{k_1}{\phi}Ox$	Ox, concentration of oxygen; D_{ox}, diffusion coefficient of oxygen ($cm^2.yr^{-1}$); ϕ, porosity (volume of the dry sediment per volume of bulk sediment)
(1.4)	$\frac{\partial U}{\partial t} = -w\frac{\partial U}{\partial z} + S(t)$	U, concentration of solid uranium; S(t) is described below; it represents the source term of the authigenic U
With		
(1.5)	$S(t) = \phi D_u \frac{U_{SW}}{d_{UU}(t)}$	D_U, diffusion coefficient of dissolved uranium ($cm^2.yr^{-1}$); U_{SW}, concentration of uranium in the ocean; $d_{UU}(t)$, depth of U uptake (cm) at time t; $d_{op}(t)$, depth of oxygen penetration (cm) at time t
(1.6)	$d_{UU}(t) = 3 \times d_{op}(t)$	

which describes the vertical distributions in sedimentary cores of chemical components. The model describes the vertical displacement of the record of a sedimentary event by a conservative component (Al), a nonconservative component (C_{org}), and a component affected by redox changes (U). This model intends to describe in how the three components record a similar sedimentation event.

2. Variables

[5] In modern sediments, the precipitation of U occurs below the depth where O_2 is consumed. Thus the depth where U accumulates corresponds to the depth where inert particles settled several thousand years ago. Conservative variables such as Al and Ti are often used as references for the variations of other chemical components [*Calvert and Pedersen*, 1993]. For instance, the vertical evolution of the U/Al ratio is used to extract the authigenic signal of a chemical component such as U from the detrital signal. Changes in this ratio can be interpreted as past variations of productivity or bottom water oxygenation. However, the Al and U signals may not be synchronous, which causes problems for the datation of a paleoceanographic event. Moreover, *Rosenthal et al.* [1995] have demonstrated that postdepositionnal redistribution of authigenic U might hamper attempts to reconstruct temporal changes in bottom water oxygen content or surface productivity from down core records of authigenic U. To describe the behavior of U and Al in buried sediments, we have used oxygen penetration into sediment as an objective criterion to identify the depth of U accumulation [*Morford and Emerson*, 1999]. This depth is calculated from the organic carbon distribution. Within the sediment, the organic carbon is a reactive element while the aluminum is an inert element. The different nature of these two elements probably influences the way by which a contemporaneous variation of incoming flux of organic carbon and aluminum may be recorded.

[6] Uranium and organic carbon buried in sediment are independent tracers of the flux of organic carbon to the seafloor [*Crusius et al.*, 1999]. The sedimentary organic carbon represents a residual part of the total quantity deposited at the sediment-water interface. U uptake depends on the redox conditions, which are driven by the quantity of organic carbon oxidized in the sediment in the absence of fluctuations in bottom water oxygen.

3. Global Structure of the Model

3.1. Biogeochemical Reactions

3.1.1. C_{org}, oxygen, and aluminum

[7] For model purposes, organic matter degradation can proceed via one of two pathways (see *Crusius et al.* [1999] for more details) (Table 1, equations (1.1)–(1.2)):

1. In the bioturbated sediment, C_{org} is mineralized at a constant rate (the one-G model of *Berner* [1980]).
2. Below the mixed layer, the degradation rate of C_{org} decreases with sediment age according to the power law of *Middelburg* [1989]. The rate is independent of redox conditions.

[8] Initially, organic matter is oxidized with oxygen according to the Redfield stoichiometry (Table 1, equation (1.3)) [*Froelich et al.*, 1979]. It allows calculation of the oxygen penetration depth, which determines the depth of U uptake. Below this depth, C_{org} mineralization continues with other oxidants.

[9] The use of the power law allows us to calculate organic carbon profiles without having to model the suboxic or anoxic oxidation of C_{org} (i.e. NO_3^-, Mn^{2+} and Fe Oxides and

SO_4^{2-}). This is of course an oversimplification of diagenesis. But for our purpose, it is a reasonable compromise that diminishes both model complexity and calculation times. Moreover, *Crusius et al.* [1999] suggests that "any uncertainties caused by leaving the pore water distributions of NO_3^-, Mn^{2+}, Fe^{2+} and SO_4^{2-} out would be compensated by a comparable uncertainty resulting from their incorporation."

3.1.2. Uranium

[10] The cycle of uranium has been studied extensively [*Wallace et al.*, 1988; *Anderson et al.*, 1989; *Thomson et al.*, 1990; *Klinkhammer and Palmer*, 1991; *Barnes and Cochran*, 1993; *Thomson et al.*, 1993]. U is conservative in oxygenated waters where it occurs in the oxidation state U (VI) [*Ku et al.*, 1977] and forms a stable, soluble anionic carbonate complex $[UO_2 (CO_3)_3]^{4-}$ [*Langmuir*, 1978]. The U concentration in seawaters is 14 nmol.kg^{-1} [*Thomson et al.*, 1990]. Under reducing conditions, the uranium is reduced to insoluble U(IV). The formation of insoluble oxides (UO_2/U_3O_8) constitutes the dominant process of particulate U enrichments in reducing marine sediments. We have computed the uptake of U in a quantitative way considering that the timescale used in this model is large enough to allow U uptake reactions to be completed. The concentration in U of the detrital fraction of marine sediments is generally around 2.7 ppm [*Thomson et al.*, 1990]. This concentration has been measured in several decarbonated samples collected in the oxic part of sediment. The concentrations in the anoxic part of the sediment are frequently higher. *Thomson et al.* [1990] demonstrated that U was supplied in the anoxic zone from the diffusive flux of dissolved U from the bottom water to the redox level where it precipitated. Numerous authors propose that the process of fixation of the uranium is introduced with the beginning of the sulfato-reduction [*Thomson et al.*, 1990; *Klinkhammer and Palmer*, 1991; *Barnes and Cochran*, 1993; *Thomson et al.*, 1993]. We have used this hypothesis in our model. The depth of sulfato-reduction is assumed to occur for a value equal to 3 times the depth of O_2 penetration (Table 1, equation (1.6)) as suggested by *Crusius et al.* [1999]. When this depth is located within the mixed layer, U uptake is assumed to occur just below. Knowing the depth of U uptake, it is possible to calculate the diffusive flux of dissolved U by considering a linear gradient of concentration between the bottom water (14 nM) and the depth of precipitation (0 nM) (Table 1, equation (1.5)). This flux represents the source term in the equation of mass conservation of the solid uranium (Table 1, equation (1.4)). The spatially distribution of this source term in the sediment is derived from comparisons to real data.

3.2. Transport

[11] The model resolves only vertical gradients; it is assumed that horizontal variations are negligible. Bioturbation is modeled as local mixing, analogous to eddy diffusion with a coefficient D_b (Table 1, equation (1.1)), and does not mix fluids against solids (i.e., intraphase mixing, [*Boudreau*, 1986a, 1986b]). Bioturbation is assumed to be constant in a layer with a thickness L. Below this depth (the fossil layer), there is no mixing only advection represented by the sedimentation rate w (cm.kyr^{-1}). Dissolved components diffuse in the pore waters according to their gradients, assuming Fick's first law modified for porosity [see e.g., *Berner*, 1980; *Ullman and Aller*, 1982; *Boudreau*, 1996].

3.3. Model Implementation

[12] To reconstruct temporal variations of the input fluxes or the dissolved elements concentration in the water overlying the sediment , the model first calculates steady state profiles, followed by a transient simulation. The simulation is run with time-variable forcing, using the steady state concentration profiles as the initial state. A few simplifications are introduced in order to assure numerical stability. Porosity and bioturbation are held constant in the mixed layer (L). Equations of particulate compounds are resolved in two steps because of the cancellation of the diffusive term at the boundary between the mixed layer and the fossil layer. Without diffusion, some finite differences schemes are unstable or cannot accurately reproduce sharp concentration fronts or gradients [*Boudreau*, 1997]. The calculation of profiles is therefore done using two different numerical schemes, the first one in the mixed layer and the second one below it (see Appendix A). The boundary conditions remain the same that those proposed in many published models: (1) at the sediment-water interface, fluxes or concentrations are imposed and (2) at the lower boundary, it is assumed that the gradients disappear (see Appendix A). In practice, this means that all degradable carbon had to be consumed within the modeled sediment column. It is a reasonable compromise used by most of modelers [*Rabouille and Gaillard*, 1991a, 1991b; *Van Cappellen et al.*, 1993; *Soetaert et al.*, 1996a, 1996b]. The validity of the solution is checked by calculating the mass balance for the whole sedimentary system. Therefore, considering that any variations of component (accumulation) must be equal to input fluxes minus sink terms and output fluxes, we have calculated the loss or gain of mass for each experiment.

4. Test and Capability of the Model

[13] In order to validate the model, predicted and measured data are compared at steady state. Another test points out the behavior of the model at nonsteady state.

4.1. Validation of the Model

4.1.1. C_{org}

[14] The organic carbon data used to validate the equation describing degradation of organic matter were collected on continental slope of the Bay of Biscay at 1000 meters depth [*Hyacinthe et al.*, 2001]. The following parameter values were used: $Fc_{org} = 50$ μmol.cm^{-2}.a^{-1}, $D_b = 0.2$ cm^2 a^{-1}, L = 1 cm et k = 10^{-2} a^{-1}. The sedimentation rate is 47 cm.ka^{-1} [*Hyacinthe et al.*, 2001]. The global mass balance of organic carbon expressed relatively to the flux at the sediment-water interface [*Rabouille and Gaillard*, 1991b] is about 0.062%. This slight deviation indicates the representativity of the predicted profile. The model successfully reproduces the general trends of the organic carbon distribution (Figure 1), using measured sedimentation and bioturbation rates and adjusting the C_{org} flux and superficial degradation rate constant. At 8 centimeters depth, the measured concentrations of carbon show a slight increase, which can arise from

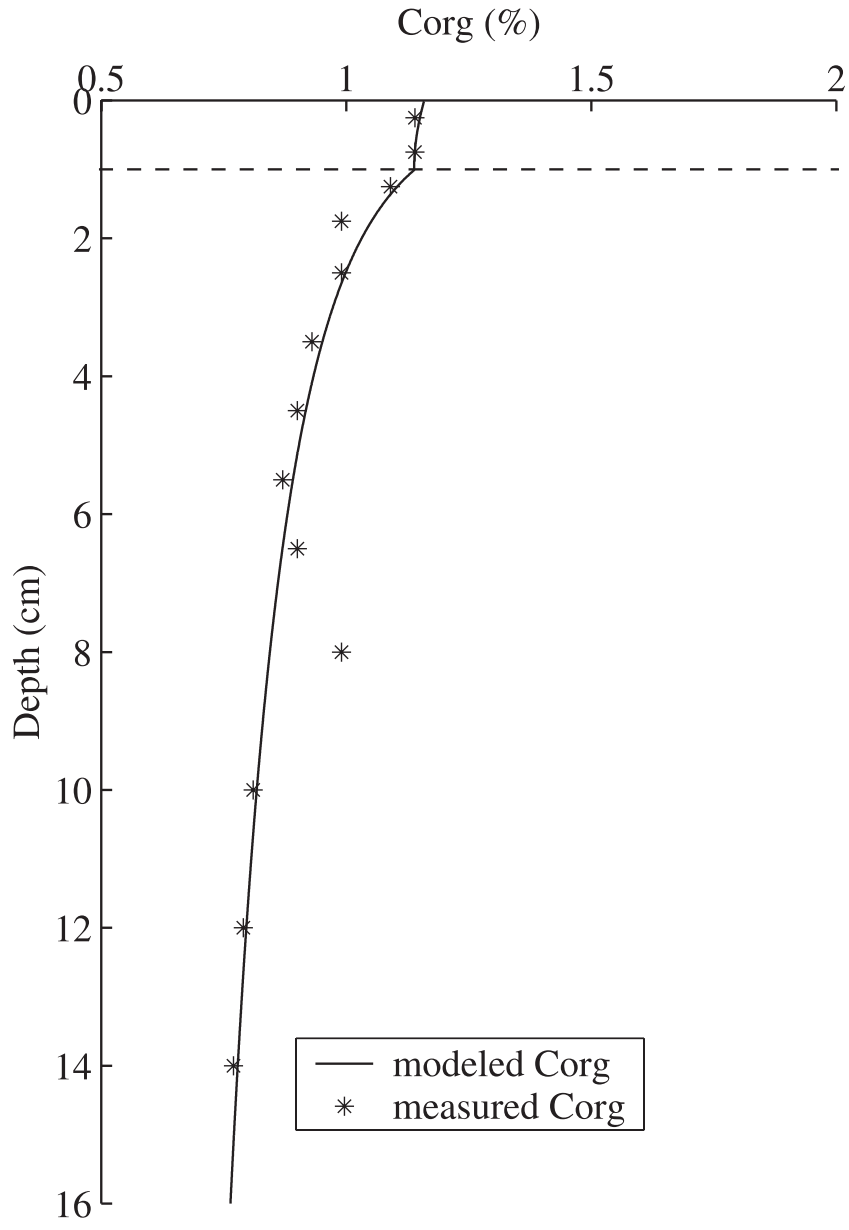

Figure 1. Comparison between measured (stars) and modeled (solid line) C_{org} profiles for sediments collected on continental slope of the Golfe of Biscaye at a depth of 1000 m. Concentrations are expressed as a fraction of dry solid. The dashed line represents the bottom of the mixed layer.

a nonlocal exchange like the infilling of a large burrow [*Boudreau*, 1986b] or from a non steady state phenomenon. The latter supposes the increase of the organic matter rain rate at the time of the deposition of sediments situated at 8 centimeters.

4.1.2. Authigenic U

[15] The output of the model correctly reproduces the data of solid uranium measured on the core 231 (Figure 2), which were collected at 3780 meters depth on the Californian continental slope [*Klinkhammer and Palmer*, 1991]. This site is representative of suboxic sediments which cover the continental margins. The following parameters were used: w = 20 $cm.ka^{-1}$, $\phi = 0.8$, $D_U = 3.3 \times 10^{-6} cm^2 s^{-1}$, $d_{UU} = 6$ *cm* and $U_{SW} = 13$ *nmol / kg* (see Table 1, equations (1.5) and (1.6), for the signification of parameters). Theses values are from measures or estimates done by *Klinkhammer and Palmer* [1991]. The molecular diffusion coefficient is corrected for the tortuosity effect [*Berner*, 1980].

4.2. Transient "Burn-Down" Enrichment

[16] We have tested the redistribution of the U signal caused by a 50% decrease in the C_{org} flux (Figure 3). The reduction in C_{org} content (Figure 3a) results in deeper penetration of pore water O_2 and other oxidants, and oxidative dissolution of previously precipitated U. As the U redox boundary deepens, a new U flux is superimposed on the initial steady state U distribution, resulting in a burn-down peak (Figure 3c). This is similar to the effect of a gravity flow

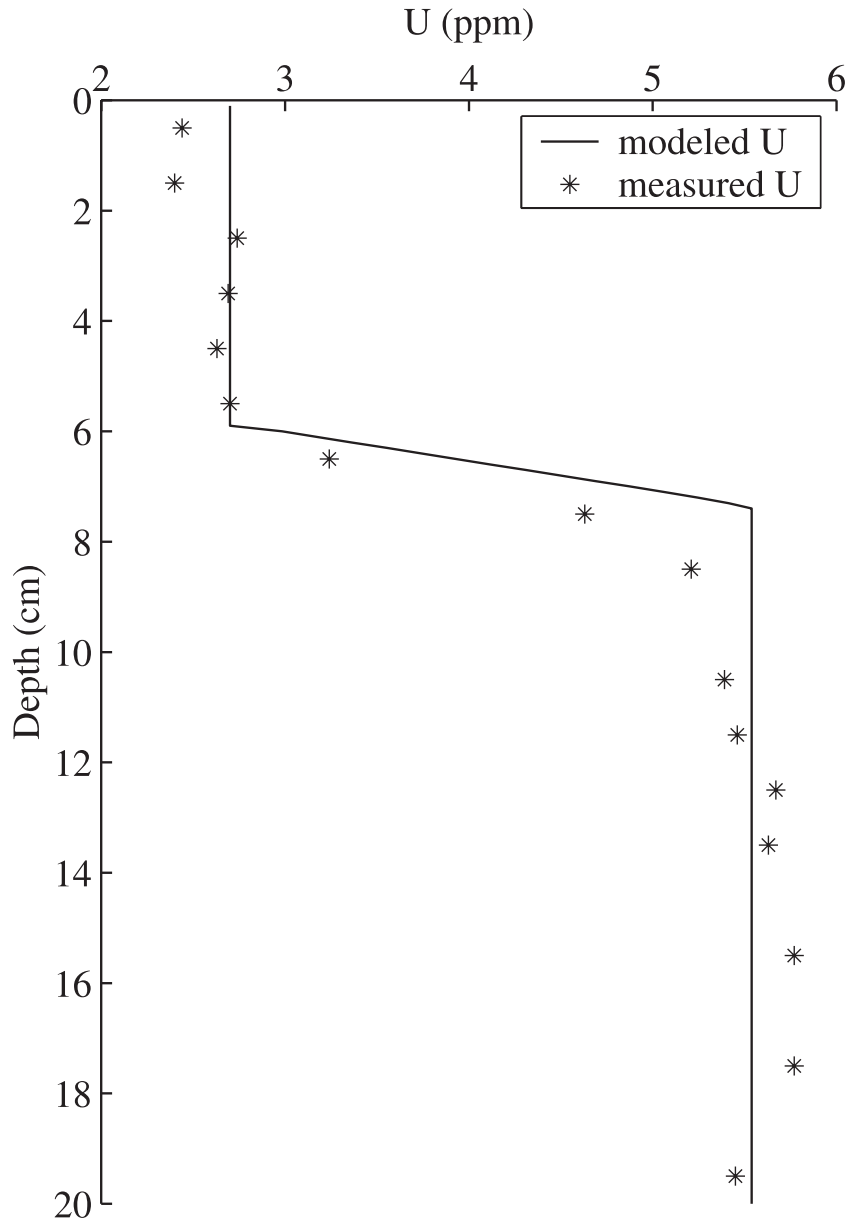

Figure 2. Comparison between measured (stars) and modeled (solid line) U profiles for sediments collected on the core 231 located on the Californian continental slope at a depth of 3780 m.

sedimentary event [*Thomson et al.*, 1993]: As the oxygen penetration depth deepens, redox-sensitive elements are redistributed, and a strong peak of U builds up below the oxic/postoxic boundary.

[17] Without taking into account the specific reactions which lead to U accumulation, these simulations of U enrichment demonstrate the capability of the model to reproduce various scenarios, from the simple steady state case to a sharp decrease of the C_{org} flux at the sediment-water interface.

5. Synchronization of Paleoceanographic Signals

5.1. Proposed Procedure

[18] Biogeochemical reactions are controlled by the following parameters (Cf. Appendix): the rate constant for C_{org} degradation used in the mixed layer (k_1), the mixed layer depth (L), and the bioturbation coefficient (D_b). The activity of organisms present in the mixed layer is mainly forced by the flux of organic matter and the bottom water oxygenation. Consequently, k_1, L and D_b depend on variations in the flux. Recent studies have shown that some of these parameters can be connected [*Boudreau*, 1994; *Tromp et al.*, 1995; *Middelburg et al.*, 1997; *Boudreau*, 1998]. For example, the rates of bioturbation and mineralization of C_{org} can be estimated from water depth [*Middelburg et al.*, 1997].

[19] The influence of early diagenesis on the recording of paleoceanographic signals is depicted in the following model simulations. We have computed the differential behavior of C_{org}, Al and U within three simple scenarios,

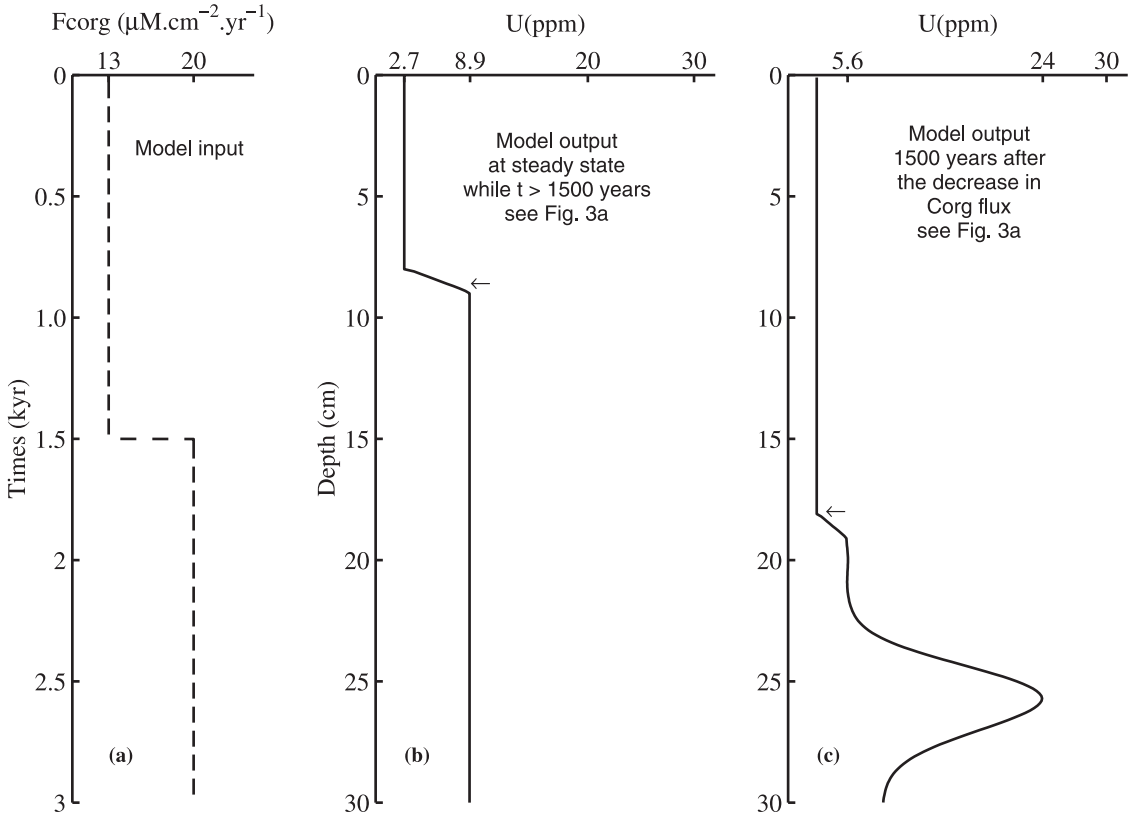

Figure 3. Example of postdepositional redistribution of authigenic uranium. (a) Distribution of C_{org} flux against times. (b) Idealized steady state sedimentary U profile. U enrichment of 6.2 ppm denoted by the arrow corresponds to a C_{org} incoming flux of 20 μmol cm^{-2} yr^{-1} (Figure 3a). (c) Idealized nonsteady state sedimentary U profile 1500 years after a 50% decrease in C_{org} flux and consequent deepening of the O_2 penetration and U reduction. A nonsteady state peak accumulates on top of the former steady state concentration The arrow denotes the new steady state U uptake depth.

to show how similar variations of the flux of organic carbon and aluminum is recorded differently in the sediment, and how these variations influence the uranium signal.

5.2. Case Studies

[20] Three cases are envisaged for which only the C_{org} and aluminum fluxes are variable. The other parameters of the model are constant. Their values are presented in Table 2. They are consistent with the values published on the early diagenesis [*Rabouille and Gaillard*, 1991b; *Tromp et al.*, 1995; *Soetaert et al.*, 1996a; *Boudreau*, 1997]. On Figures 4, 5, and 6, two graphs are presented. The left one gives the inputs of the model (flux against time) and the right one gives the outputs of the model (profiles of organic carbon, aluminum and uranium against depth). The vertical scales of time and depth are chosen so that, when transport is only driven by burial, a 1000 years old increase of input flux is recorded at 10 cm depth. For all the cases presented below, an average value of 0.23% of mass of elements in the sediment were created or lost over the entire 6000 year-run.

Table 2. Values of the Parameters Used for the Three Scenarios Tested

Parameter	Value
D_b, cm^2 yr^{-1}	0.2
L, cm	7
k_1, yr^{-1}	0.008
Ox_{BW}, μmol L^{-1}	200
W, cm kyr^{-1}	10
ϕ	0.8

5.2.1. Case 1

[21] In the first case, the C_{org} and aluminum fluxes were set at 13 and 4 μmol.cm^{-2}.yr^{-1}, respectively, beginning with year 6000 (Figure 4a). In year 3500, both fluxes were increased by 50%. Figure 4b shows C_{org}, Al and U profiles for the 6000 years time interval. The arrow indicates the depth where the transition should be located in the absence of mixing. The contrast between the C_{org} and Al distributions is striking. On the C_{org} profile, a transition to higher values is located around 40 cm. The recording of the same episode by the aluminum is different. The transition spreads over a 20 cm depth interval and is located around 38 cm. Thus there is a 2 cm spatial offset between the two

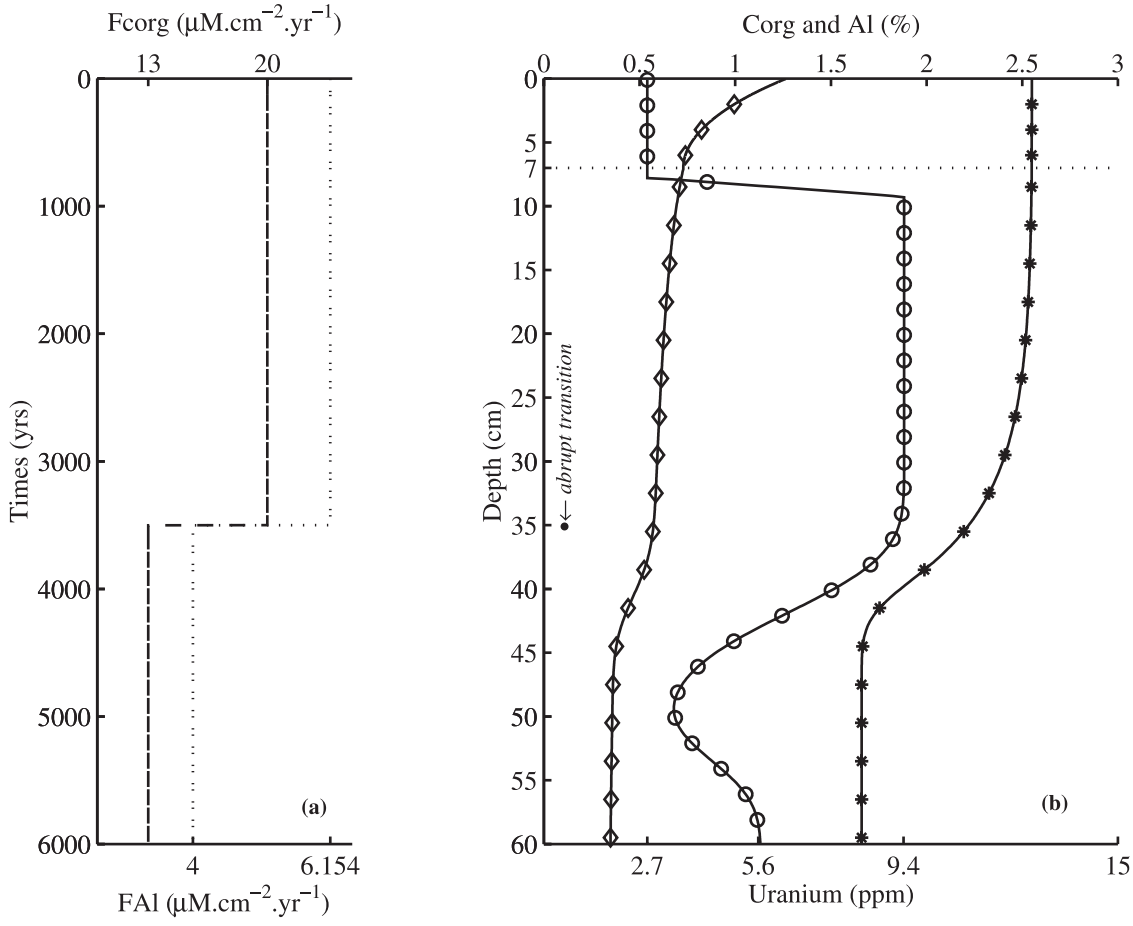

Figure 4. (a) Time series of the C_{org} flux (dashed line) and the Al flux (dotted line). (b) Distributions of C_{org} (diamonds), Al (stars) and U (circles) against depth in the sediment. Theses profiles result from the evolution of the input fluxes depicted on the left side. All the other parameters of the model are fixed (Table 2). The straight dotted line represents the bottom of the bioturbated layer. The C_{org} and Al are expressed as a fraction of dry solids.

transitions. This offset distributions may be explained by considering the residence time of each component within a given layer. The residence time inside the mixed layer is 190 years for C_{org} and 700 years for aluminum. Aluminum reacts slower to a disturbance of the flux than the organic carbon. Indeed, following the fast disturbance, the most reactive element C_{org} comes back to a steady state faster than the inert element Al (*Albarède*, 1995).

[22] The steady state concentration of U for conditions imposed from 3500 years to present is 9.4 ppm, which is measured from 8 to 30 cm depth. Below U concentration decreases to a minimum value of 4.3 ppm at 49 cm depth. Then, it increases again to a steady state concentration of 5.6 ppm below 58 cm. To explain the uranium distribution, we have to look at the evolution of oxygen penetration (Figure 7). The oxic layer depth was 5.94 cm from 6000 to 3500 years and 2.63 cm from year 2800 to 0. Between year 3500 and 3400, the oxic layer decreases quickly from 5.94 to 3.57 cm, and then more slowly to a new steady state depth of 2.63 cm in year 2800. During this transition period, the U uptake depth rose from 17.82 cm to 10.71 cm (three time the oxic layer depth) in 100 years. During the quick ascent of the U fixation depth, only small amounts of authigenic U accumulated. This explains the minimum observed at 49 cm depth.

[23] The first case leads to these implications: (1) In a high-resolution record, there is a weak time lag between a reactive and an inert component, responding to an identical event. (2) The three studied components record a same episode over different sediment thickness. In our example, uranium records the transition as a minimum in an 18 cm thick layer, the organic carbon records the same variation in a 8 cm layer, and aluminum spreads the transition over 20 cm.

5.2.2. Case 2

[24] The maximal and minimal values of the C_{org} and Al fluxes are the same as in case 1, but the fluxes were constant at 13 and 4 μmol.cm^{-2}.yr^{-1} over the entire period except between years 2000 and 1800, when a symmetrical peak was introduced with maximum values of 20 and 6.154 μmol.cm^{-2}.yr^{-1} in year 1900 (Fig 6a). The 200 yearlong event is not significantly recorded on the profiles

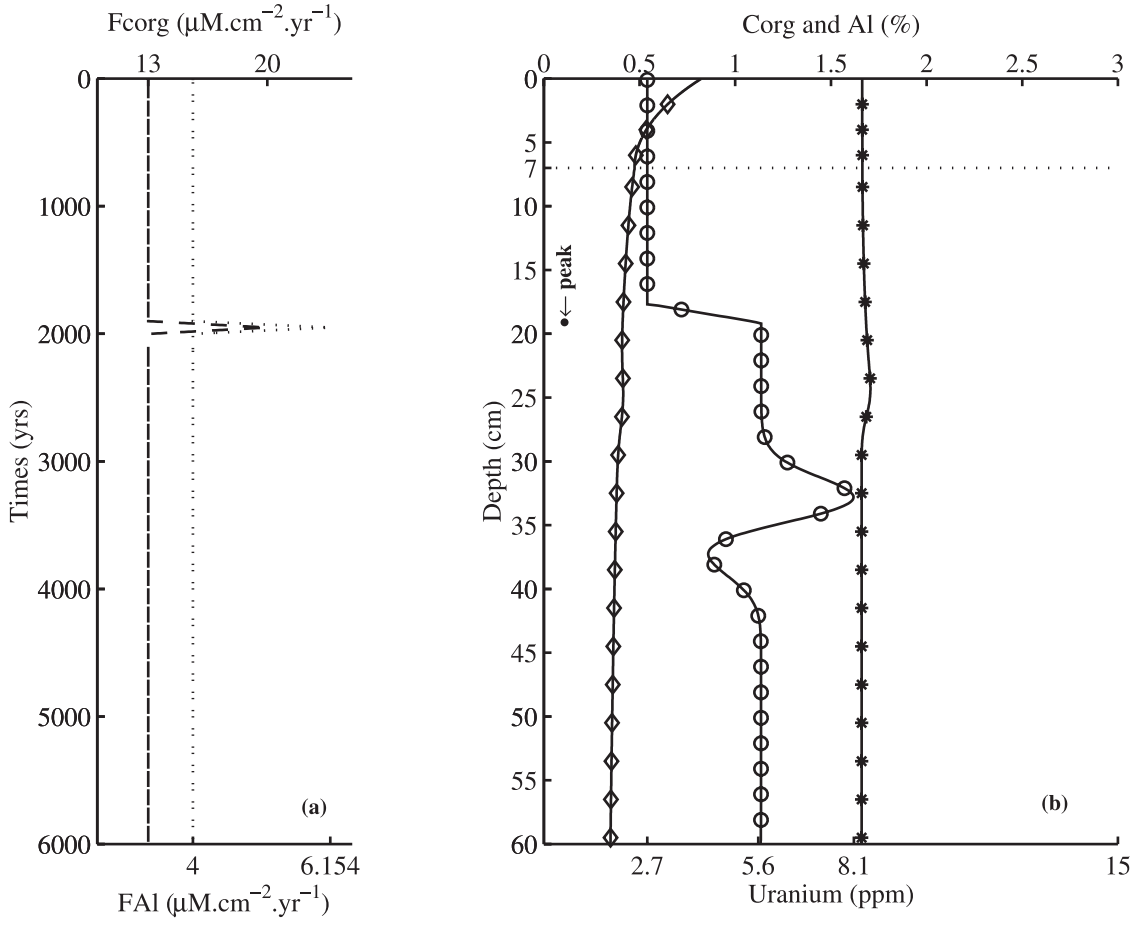

Figure 5. Same as Figure 4.

of C_{org} and Al (Figure 5b), because the signals are smoothed by mixing in the bioturbated layer. Bioturbation eliminates high frequency variations. Uranium, however, preserves a record of the signal (Figure 5b). The steady state concentration of U in the anoxic sediment is 5.6 ppm. The short perturbation yields a maximum value of 8.1 ppm at 33 cm depth and a minimum of 4 ppm at 37.4 cm. The minimum situated at 37.4 cm is connected to the increase of the C_{org} flux between years 2000 and 1900, and finds its explanation in the case study 1. The maximum results from the decrease of the C_{org} flux between years 1900 and 1800, it is a peak of remobilization. This situation shows that the U profiles must be interpreted with caution, in terms of temporal evolution a peak of C_{org} flux produces a minimum then a maximum of uranium situated between 42 and 28 cm. In terms of paleoclimatic interpretations of deep-sea records, this thickness represents 1400 years although it only reflects a single episode of only 200 years duration. The U maximum is situated more than 10 cm below the depth corresponding to the event, i.e. 1000 years earlier.

5.2.3. Case 3

[25] In the third scenario, which is similar to case 2, the peak in the sedimentation fluxes is broadened and extends over a period of 1000 years from year 4000 to year 3000 (Figure 6a). On the Figure 6b, the arrow indicates the depth in the sediment, 35 cm, at which the maximum of fluxes should have influenced geochemical profiles in the absence of bioturbation. The contrast between the C_{org} and Al distributions is remarkable (Figure 6b). On the C_{org} profile, a small increase is situated at 40.5 cm whereas on the Al profile, a maximum is visible at 38.5 cm. As in case 2, bioturbation smoothes the slow variations but does not eliminate them. The 2 cm shift is explained by the different residence times of Al and C_{org} in the mixed layer as described in case 1. The U profile shows a minimum of 3.7 ppm at 53.8 cm and a maximum of 13.9 ppm at 44.3 cm (Figure 6b). The steady state concentration of U in the anoxic sediment is 5.6 ppm. Consistently with case 2, the spatial offset between the time of the maximum of C_{org} flux (see the arrow) and the U maximum is about 10 cm. Moreover, the event of 1000 years generates U profile variations spreading over more than 20 cm in the sediment. We can conclude that U profiles must be interpreted with caution in terms of temporal evolution.

[26] None of the three paleoceanographic signals modeled records the same episode at an identical depth.

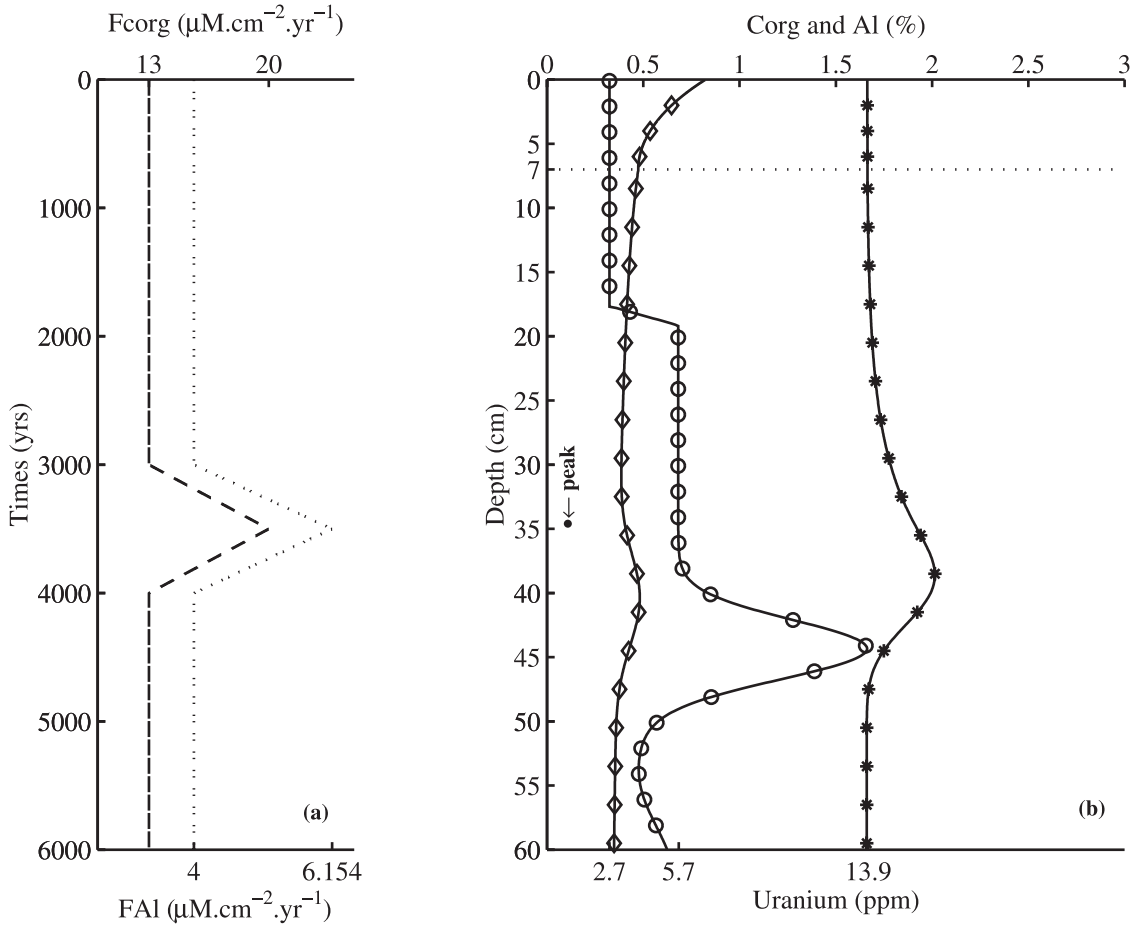

Figure 6. Same as Figure 4.

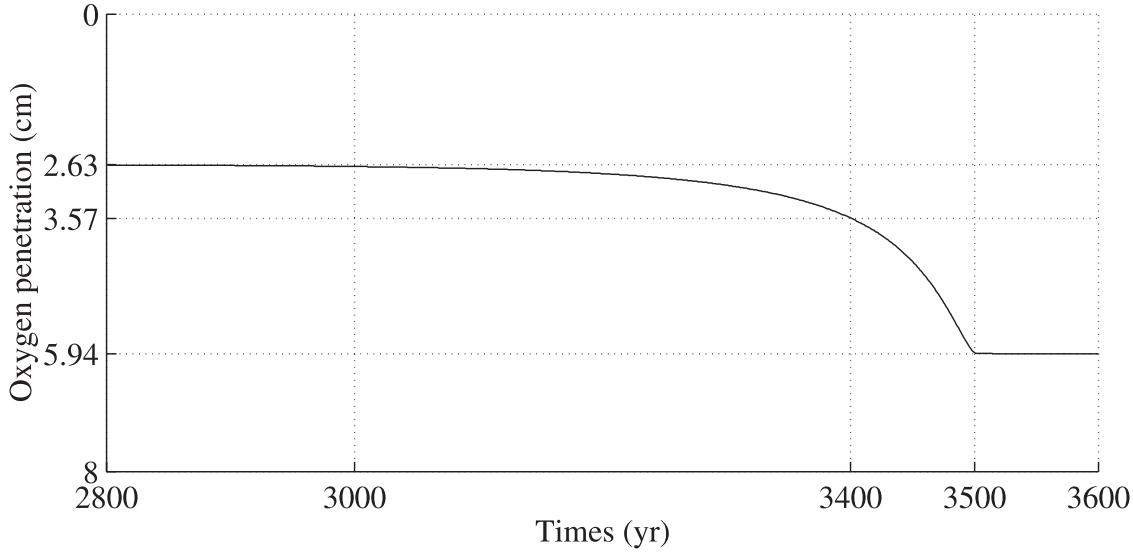

Figure 7. Evolution of the oxygen penetration depth following the increase in C_{org} and Al flux imposed to the boundary.

6. Conclusion

[27] The simple model we have built can be used to gain insight into the behavior of paleoceanographic signals. The dynamic description of coupled transport processes and redox-front movements of components with different reactivity and/or chemical properties in a sediment has allowed us to identify some uncertainties that will affect the interpretation of paleoceanographic time series.

[28] The model calculations show that it can be difficult to interpret uranium profiles in terms of temporal evolution. However, as the model shows, the interpretation of U distributions can be improved. For example, a minimum of U does not necessarily mean a deep depth of U uptake. It could equally well be caused by a rapid variation of the oxygen penetration depth as the flux or the bottom water composition change.

[29] The simulations performed in the present study also illustrate the nonlinearity of the sedimentary response to variations in the sedimentation input fluxes. A synchronous change in the C_{org} and Al fluxes is not recorded at exactly the same depth when the surface sediment undergoes mixing, because of their specific behavior in the mixed layer. Signals of short duration are not recorded in the C_{org} and Al profiles because of the smoothing by bioturbation, whereas U, when it precipitates below the mixed layer preserves a record of this episode. Multiproxy approaches are necessary in order to reduce the uncertainties when interpreting paleoceanographic time series.

[30] Finally, although this study has focused on simple scenarios where we have pointed out the limitations of interpreting the paleoceanographic record without a multiproxy approach, the model can also be used in very large set of perturbation, and may be a powerful tool to predict C_{org}, Al and U profiles for real perturbations (HE, D/O) and also to quantify spatial offsets.

Appendix A: Numerical Approximation

A1. Mixed Layer

[31] The spatial derivatives (diffusion and advection) of the partial differential equations are approximated by means of centered space terms which are second order accurate. The temporal derivative is treated using forward time. The space variable z is divided into n sediment layers of thickness dz with L = n * dz. Thus, for organic carbon the difference equation (equation (1.1) in Table 1) becomes:

$$\frac{G_i^{k+1}-G_i^k}{\Delta t} = D_B\left\{\frac{G_{i+1}^{k+1}-2G_i^{k+1}+G_{i-1}^{k+1}}{\Delta z^2}\right\} - w\left\{\frac{G_{i+1}^{k+1}-G_{i-1}^{k+1}}{2\Delta z}\right\} - kG_i^{k+1} \quad \text{(A1)}$$

The equivalent scheme is used for Al and O_2.

[32] For the upper boundary of a dissolved sediment component (z = 0), the concentration in the bottom water is imposed:

$$C_{z=0} = C_{BW} \quad \text{(A2)}$$

The upper boundary condition for solid substances is imposed as **a** flux (example for the organic carbon):

$$F_{Corg}^{k+1} = -D_B\left\{\frac{G_1^{k+1}-G_{-1}^{k+1}}{2\Delta z}\right\} + wG_0^{k+1} \quad \text{(A3)}$$

At the lower boundary, it is assumed that the gradients disappear:

$$\frac{G_n^{k+1}-G_{n-1}^{k+1}}{\Delta z} = 0 \quad \text{(A4)}$$

A2. Fossilized Layer

[33] In the case of the advection-reaction equations as $\frac{\partial G}{\partial t} = -w\frac{\partial G}{\partial z} - k(t)G$, the Leapfrog differencing scheme is the most commonly used [*Boudreau*, 1997]:

$$\frac{G_i^{k+1}-G_i^{k-1}}{\Delta t} = -w\frac{G_{i+1}^k-G_{i-1}^k}{\Delta z} - k_iG_i^k \quad \text{(A5)}$$

[34] Leapfrog formulas are precise and do not generate numerical diffusion. Nevertheless, they can infer small oscillations when a large gradient is introduced. In order to model and to preserve abrupt variations of particular input flux, the Sweby scheme [*Sweby*, 1984] is more appropriate to our constraints. It introduces a correction that adjusts local diffusion quantity and allows large gradients to be preserved. Its shape is the following:

$$G_i^{k+1} = G_i^k - w\frac{\Delta t}{\Delta z}\left\{G_i^k - G_{i-1}^k\right\} + w\frac{\Delta t}{2\Delta z} \cdot \left\{\Phi(r_i)\nu_i\left(G_{i+1}^k - G_i^k\right) - \Phi(r_{i-1})\nu_{i-1}\left(G_i^k - G_{i-1}^k\right)\right\} \quad \text{(A6)}$$

Where in the model

$$\nu_i = 1 \forall i \quad \text{(A7)}$$

$$r_i = \frac{G_i^k - G_{i-1}^k}{G_{i+1}^k - G_i^k} \quad \text{(A8)}$$

and finally:

$$\Phi(r_i) = \begin{cases} 0 & if\ r_i < 0 \\ r_i & if\ r_i \le 1 \\ 1 & if\ r_i > 1. \end{cases} \quad \text{(A9)}$$

As for all explicit method in time, the following condition has to be checked (Courant number):

$$\frac{w\Delta t}{\Delta z} \le 1 \quad \text{(A10)}$$

[35] **Acknowledgments.** We thank Bjorg Sundby and Keith Rodgers for the improvement of the English language. We thank C. Rabouille, P. Martinez, and X. Giraud for assistance in the field and stimulating discussion. The text benefited greatly from reviews by two anonymous reviewers and L. Peterson.

References

Albarède, F., *Introduction to Geochemical Modeling*, 543 pp., Cambridge Univ. Press, New York, 1995.

Aller, R. C., Bioturbation and manganese cycling in hemipelagic sediments, *Philos. Trans. R. Soc. London, Ser. A*, *331*, 51–68, 1990.

Anderson, R. F., M. Q. Fleisher, and A. P. LeHuray, Concentration, oxidation state, and particulate flux of uranium in the Black Sea, *Geochim. Cosmochim. Acta*, *53*, 2215–2224, 1989.

Bard, E., M. Arnold, J. Duprat, J. Moyes, and J.-C. Duplessy, Reconstruction of the last deglaciation: Deconvolved records of $\delta^{18}O$ profiles, micropaleontological variations and accelerator mass spectrometric ^{14}C dating, *Clim. Dyn.*, *1*, 101–112, 1987.

Barnes, C. E., and J. K. Cochran, Uranium geochemistry in estuarine sediments: Controls on removal and release processes, *Geochim. Cosmochim. Acta*, *57*, 555–569, 1993.

Berger, W. H., and G. R. Health, Vertical mixing in pelagic sediments, *J. Mar. Res.*, *26*, 135–143, 1968.

Berner, R. A., *Early Diagenesis: A Theoretical Approach*, 241 pp., Princeton Univ. Press, Princeton, N. J., 1980.

Boudreau, B. P., Mathematics of tracer mixing in sediments, I, Spatially-dependent, diffusive mixing, *Am. J. Sci.*, *286*, 161–198, 1986a.

Boudreau, B. P., Mathematics of tracer mixing in sediments, II, Non-local mixing and biological conveyor-belt phenomena, *Am. J. Sci.*, *286*, 199–238, 1986b.

Boudreau, B. P., Is burial velocity a master parameter for bioturbation?, *Geochim. Cosmochim. Acta*, *58*, 1243–1249, 1994.

Boudreau, B. P., The diffusive tortuosity of fine-grained unlithified sediments, *Geochim. Cosmochim. Acta*, *60*, 3139–3142, 1996.

Boudreau, B. P., *Diagenetic Models and Their Implementation*, 414 pp., Springer-Verlag, New York, 1997.

Boudreau, B. P., Mean mixed depth of sediments: The wherefore and the why, *Limnol. Oceanogr.*, *43*, 524–526, 1998.

Calvert, S. E., and T. F. Pedersen, Geochemistry of Recent oxic and anoxic marine sediments: Implications for the geological record, *Mar. Geol.*, *113*, 67–88, 1993.

Colodner, D., J. Edmond, and E. Boyle, Rhenium in the Black Sea: Comparison with molybdenum and uranium, *Earth Planet. Sci. Lett.*, *131*, 1–15, 1995.

Crusius, J., S. Calvert, T. Pedersen, and D. Sage, Rhenium and molybdenum enrichments in sediments as indicators of oxic, suboxic and sulfidic conditions of deposition, *Earth Planet. Sci. Lett.*, *145*, 65–78, 1996.

Crusius, J., T. F. Pedersen, S. E. Calvert, G. L. Cowie, and O. Tadamichi, A 36 kyr geochemical record from the Sea of Japan of organic matter flux variations and changes in intermediate water oxygen concentrations, *Paleoceanography*, *14*, 248–259, 1999.

Dhakar, S. P., and D. J. Burdige, A coupled, nonlinear steady-state model for early diagenetic processes in pelagic marine sediments, *Am. J. Sci.*, *296*, 296–330, 1996.

Froelich, P. N., G. P. Klinkhammer, M. L. Bender, N. A. Luedke, G. R. Heath, D. Cullen, P. Dauphin, D. Hammond, B. Hartman, and V. Maynard, Early oxidation of organic matter in pelagic sediments of the eastern equatorial Atlantic: Suboxic diagenesis, *Geochim. Cosmochim. Acta*, *43*, 1075–1090, 1979.

Gobeil, C., R. W. Macdonald, and B. Sundby, Diagenetic separation of cadmium and manganese in suboxic continental margin sediments, *Geochim. Cosmochim. Acta*, *61*, 4647–4654, 1997.

Guinasso, N. L. J., and D. R. Schink, Quantitative estimates of biological mixing rates in abyssal sediments, *J. Geophys. Res.*, *80*, 3032–3043, 1975.

Hyacinthe, C., P. Anschutz, P. Carbonel, J. M. Jouanneau, and F. J. Jorissen, Early diagenetic processes in the muddy sediments of the Bay of Biscay, *Mar. Geol.*, *177*, 111–128, 2001.

Jorissen, F. J., H. C. De Stiger, and J. G. V. Widmark, A conceptual model explaining benthic foraminiferal microhabitats, *Mar. Micropaleontol.*, *26*, 3 –15, 1995.

Klinkhammer, G. P., and M. R. Palmer, Uranium in the oceans: Where it goes and why, *Geochim. Cosmochim. Acta*, *55*, 1799–1806, 1991.

Ku, T. L., K. G. Knauss, and G. G. Mathieu, Uranium in open ocean: Concentration and isotopic composition, *Deep Sea Res.*, *24*, 1005–1017, 1977.

Langmuir, D., Uranium solution-mineral equilibria at low temperatures with applications to sedimentary ore deposits, *Geochim. Cosmochim. Acta*, *42*, 547–569, 1978.

Middelburg, J. J., A simple rate model for organic matter decomposition in marine sediments, *Geochim. Cosmochim. Acta*, *53*, 1577–1581, 1989.

Middelburg, J. J., K. Soetaert, and P. M. J. Herman, Empirical relationships for use in global diagenetic models, *Deep Sea Res., Part I*, *44*(2), 327–344, 1997.

Morford, J. L., and S. Emerson, The geochemistry of redox sensitive trace metals in sediments, *Geochim. Cosmochim. Acta*, *63*, 1735–1750, 1999.

Rabouille, C., and J. F. Gaillard, A coupled model representing the deep-sea organic carbon mineralization and oxygen consumption in surficial sediments, *J. Geophys. Res.*, *96*, 2761–2776, 1991a.

Rabouille, C., and J. F. Gaillard, Towards the EDGE: Early diagenetic global explanation, A model depicting the early diagenesis of organic matter, O_2, NO_3, Mn and PO_4, *Geochim. Cosmochim. Acta*, *55*, 2511–2525, 1991b.

Rosenthal, Y., P. Lam, E. A. Boyle, and J. Thomson, Authigenic cadmium enrichments in suboxic sediments: Precipitation and post-depositional mobility, *Earth Planet. Sci. Lett.*, *132*, 99–111, 1995.

Soetaert, K., P. M. J. Herman, and J. J. Middelburg, Dynamic response of deep-sea sediments to seasonal variations: A model, *Limnol. Oceanogr.*, *41*, 1651–1668, 1996a.

Soetaert, K., P. M. J. Herman, and J. J. Middelburg, A model of early diagenetic processes from the shelf to abyssal depths, *Geochim. Cosmochim. Acta*, *60*, 1019–1040, 1996b.

Sweby, B. K., High resolution schemes using flux limiters for hyperbolic conservation laws, *J. Numer. Anal.*, *21*, 995–1011, 1984.

Thomson, J., H. E. Wallace, S. Colley, and J. Toole, Authigenic uranium in Atlantic sediments of the last glacial stage: A diagenetic phenomenon, *Earth Planet. Sci. Lett.*, *98*, 222–232, 1990.

Thomson, J., N. C. Higgs, I. W. Croudace, S. Colley, and D. J. Hydes, Redox zonation of elements at an oxic/post-oxic boundary in deep-sea sediments, *Geochim. Cosmochim. Acta*, *57*, 579–595, 1993.

Tromp, T. K., P. Van Cappelen, and R. M. Key, A global model for the early diagenesis of organic carbon and organic phosphorus in marine sediments, *Geochim. Cosmochim. Acta*, *59*, 1259–1284, 1995.

Ullman, W. J., and R. C. Aller, Diffusion coefficients in nearshore marine sediments, *Limnol. Oceanogr.*, *27*, 552–556, 1982.

Van Cappellen, P., J. F. Gaillard and C. Rabouille, Biogeochemical transformations in sediments: Kinetic models of early diagenesis, in *Interactions of C, N, P and S Biogeochemical Cycles and Global Change, NATO ASI Ser., Ser. I*, vol. 4, pp. 401–445, Springer-Verlag, New York, 1993.

Wallace, H. E., J. Thomson, T. R. S. Wilson, P. P. E. Weaver, N. C. Higgs, and D. J. Hydes, Active diagenetic formation of metal-rich layers in N. E. Atlantic sediments, *Geochim. Cosmochim. Acta*, *52*, 1557–1569, 1988.

Wheatcroft, R. A., Experimental tests for particle size-dependent bioturbation in the deep ocean, *Limnol. Oceanogr.*, *37*, 90–104, 1992.

P. Anschutz, P. Bertrand, and P. Lecroart, DGO-UMR 5805, Université Bordeaux 1, 33405 Talence, France.

Y. Donnadieu, Laboratoire des Sciences du Climat et de l'Environnement, UMR CNRS-CEA, CEA Saclay, Orme des Merisiers, Bat. 709, 91191 Gif-sur-Yvette cedex, France. (tiphe@lsce.saclay.cea.fr)